Computational and Theoretical Chemistry 964 (2011) 248–256

Contents lists available at ScienceDirect

Computational and Theoretical Chemistry

journal homepage: www.elsevier.com/locate/comptc

Theoretical studies on the gas phase reaction mechanisms and kinetics of glyoxal with HO_2 with water and without water

Bo Long [a,*], Wei-jun Zhang [b], Xing-feng Tan [c], Zheng-wen Long [d], Yi-bo Wang [e], Da-sen Ren [a]

[a] College of Computer and Information Science, Guizhou University for Nationalities, Guiyang 550025, China
[b] Laboratory of Environment Spectroscopy, Anhui Institute of Optics and Fine Mechanics, Chinese Academy of Sciences, Hefei 230031, China
[c] College of Photo-Electronics, Chongqing University of Posts and Telecommunications, Chongqing 400065, China
[d] Department of Physics, Guizhou University, Guiyang 550025, China
[e] Key Laboratory of Guizhou High Performance Computational Chemistry, Department of Chemistry, Guizhou University, Guiyang 550025, China

ARTICLE INFO

Article history:
Received 16 August 2010
Received in revised form 27 December 2010
Accepted 1 January 2011
Available online 11 January 2011

Keywords:
Glyoxal
HO_2
Reaction mechanism
Quantum chemical calculations

ABSTRACT

The quantum chemical methods are employed to investigate the reactions of glyoxal with the HO_2 radical and the HO_2 and H_2O. There are twelve complexes found herein, whose stabilized energies are in the range of −3.8 kcal/mol to −12.3 kcal/mol. The calculated results predict that the proton coupled electron transfer process is the most favorable in the reactivity of the HO_2 radical with glyoxal due to the low energy barrier of 5.4 kcal/mol. In addition, the barriers in the reaction glyoxal with the formed $HO_2\cdots H_2O$ complex are so high that the processes are unlikely to occur in the atmosphere, whereas the energy barriers of the HO_2 reaction with the complexes formed between glyoxal and water are decreased. Additionally, the rate constant of the proton coupled electron transfer process is computed to be 2.83×10^{-16} cm^3 molecule^{-1} s^{-1} at 298 K using the transition state theory with Eckart correction, which agrees well with the experimental data. It is noted that the rate constants of the water-catalyzed glyoxal reaction with HO_2 is increased about 10 times greater than the naked reaction $HO_2 + (CHO)_2$.

1. Introduction

Glyoxal $(HCO)_2$, is the simplest α-dicarbonyl intermediate product produced form the atmospheric oxidation of the biogenic [1–3] and anthropogenic precursors [4–8] primarily emitted from biomass burning [6] and car exhaust [7,8]. Therefore, in urban area [9] the concentrations of glyoxal are elevated, which has been observed. Glyoxal is of great significance in atmospheric chemistry because it can be utilized as tracer for isoprene and other biogenic emissions, makes the major contribution to the formation of the secondary organic aerosol (SOA) [10–14] and has an effect on HO_x ($HO + HO_2$) budget. The atmospheric fate of glyoxal is short with on the order of hours. The major removal processes of glyoxal are determined by the gas-phase photolysis [15–19] with $\tau_{Phot} \approx 2$ to 3 h [15,16] in the UV region and blue region of the visible spectrum, the reaction with the OH radical equal to ~24 h [15]and aerosol absorption [1,2,12,13,20–24] responsible for the formation of one sixth of secondary organic aerosol (SOA) observed at a Mexico City field site [2].

As for the reaction of glyoxal with the HO_2 radical, there is only one experimental report [25] with a rate constant of 5.00×10^{-16} cm^3 molecule^{-1} s^{-1} at 298 ± 2 K, which indicates that the reaction is quite slow and is of minor importance in the atmosphere. However, Anglada et al. [26] computed the reaction of HO_2 with formaldehyde, which shows that the reaction with a rate constant of 9.29×10^{-14} cm^3 molecule^{-1} s^{-1} plays an important role in the atmospheric chemistry. Thus, we feel that a theoretical study of the reaction HO_2 with glyoxal is of great necessity because there are many similarly structural features between formaldehyde and glyoxal that both of the structures of the HCHO and $(CHO)_2$ involve the formyl radical (HCO). In addition, the 30% of all HO_2 [27,28] is in the complex form at 298 K and the $HO_2\cdots H_2O$ complex can accelerate the rate constants in the reactions of HO_2 self-reaction [29], SO_3 [30] and CF_3OH [31] with the $HO_2\cdots H_2O$ complex.

Thus, in the present study, the ab initio methods and the conventional transition state theory (TST) are employed to investigate the reactions of the naked HO_2 radical with glyoxal and HO_2 with glyoxal with the single water molecule added. As far as we know, there is the first theoretical study on he the title reaction. The goal is to elucidate the reaction mechanisms of the naked HO_2 radical and the HO_2 radical added water with glyoxal and to determine whether the water-catalyzed process of the reaction is more important than the corresponding non-catalytic process for the split of the glyoxal from the energetic and kinetic points of view.

* Corresponding author.
E-mail address: wwwltcommon@sina.com (B. Long).

2210-271X/$ - see front matter Crown Copyright © 2011 Published by Elsevier B.V. All rights reserved.
doi:10.1016/j.comptc.2011.01.003

2. Theoretical methods

The electronic structure calculations were performed using the Gaussian 03 [32] software. The geometries of all the reactants, pre-reactive complexes, transition states and products were optimized at the B3LYP/6-311++G(d,p) level of theory and the corresponding frequencies of the optimized geometries were computed at the same level to prove the characters of the transition states with one imaginary frequency and the stationary points with positive frequencies because Anglada [26] studied the similar reaction of HO_2 with HCHO using the B3LYP functional, which is in excellent agreement with the experimental data. In order to obtain the relative energies reliably, single point energies were performed using the CCSD(T)/6-311++G(d,p) method at the B3LYP-optimized geometries. In these computations, the value of T1 diagnostic [33,34] in the CCSD wave function was considered to evaluate the reliability of these computations with respect to a possible multireference feature of the wave function at the stationary points. Moreover, as for the complexes founded in this study, the basis set superposition error (BSSE) was calculated using the counterpoise method by Boys and Bernardi [35] at the CCSD(T)/6-311++G(d,p) and B3LYP/6-311++G(d,p) levels of theory to assess the energetic stability of the complexes better. It is noted that the complexes formed between glyoxal and $HO_2\cdots H_2O$, $(CHO)_2\cdots H_2O$ and HO_2 are considered to be three fragments. In addition, the H-bond natures in this investigation were analyzed in terms of the atoms in molecules (AIM) theory by Bader [36], which was carried out in AIM2000 [37–39]. If necessary, the intrinsic reaction coordinate (IRC) [40,41] was employed at the B3LYP/6-311++G(d,p) level of theory to verify the transition states connected with the desired reactants and products. Finally, the rate constant was calculated using the transition state theory with Eckart correction, which was executed in the TheRate program [42].

3. Results and discussion

3.1. Reactants and pre-complexes

The optimized parameters of reactants are shown in Fig. 1, which is in good agreement with the experimental [43,44] data and theoretical results [45,46], indicating the selected method is reliable to characterize the reaction system. As the pre-reactive complexes are of great importance in the processes of the chemical reaction and are the incipient step of the reaction, the complexes between glyoxal and HO_2, glyoxal and $HO_2\cdots H_2O$, $(CHO)_2\cdots H_2O$ and HO_2 are located as presented in Figs. 1 and 2. There are three complexes (C1, C2 and C3) found between glyoxal and HO_2. From Fig. 1, the complex C1 with the bind energy of −3.8 kcal/mol from Table 1 is a five-membered ring structure with one hydrogen between O4···H9 bond interaction and one van der Waals interaction between C5···O7, which is similar to the complex between formaldehyde [26] and HO_2. It is noted that due to the lack of the dispersion correction for the B3LYP, the binding energy of the C1 may be underestimated and Table 1 tells that the BSSE correction using CCSD(T) theoretical method is overestimated. Combined with the higher level to study the HO_2 and HCHO [26], we feel that the reported binding energy of C1 is reasonable and reliable. Therefore, the binding energies of the complexes reported herein are based on the CCSD(T)//B3LYP/6-311++G(d,p) level plus the BSSE correction at the B3LYP/6-311++G(d,p) level. The geometrical parameters show that the O4···H9 bond distance is 1.763 Å and the C5···O7 bond length is 2.583 Å, reflecting that the O4···H9 interaction is stronger than the C5···O7 interaction, which is confirmed by the topological properties of the wave function because the bond strengthen correlates with the charge density (ρ) at the bond critical points (bcps) in terms of the AIM theory by Bader (see Table 2) [36,47]. In addition, according to the AIM theory, Laplacian of the electron density ($\Delta^2\rho$), kinetic electron density (G), potential electron energy density (V), and the total electron energy density (H), which is sum of the kinetic electron density and the potential electron density at the bcps reveal the nature of the interactions. It is pointed out that the H is negative and the $\Delta^2\rho$is positive, reflecting the interaction is partially covalent, whereas H is positive and the $\Delta^2\rho$ is positive, revealing that the interaction is only electrostatic interaction in nature. The complexes C2 reported in the literature [48] and C3 are the seven-membered ring structure and six-membered ring structure, where all atoms lie in the same plane with two hydrogen bonds involved. It is noted that the CCSD(T)//B3LYP/6-311++G(d,p) method cannot correctly describe the complex C3 binding energy because the calculated geometrical parameters show that the complex C2 is more stable than the complex C3. Moreover, the B3LYP stabilized energy also proves this point because the stabilization energy of C2 is 0.1 kcal/mol lower than the corresponding C3. Additionally, the stabilized energy of C2 is found to be 5.2 kcal/mol at the CCSD(T)//B3LYP/6-311++G(d,p) level of theory, which agrees well with the value of 5.1 kcal/mol by Francisco [48].

As for the ternary complexes between glyoxal and $HO_2\cdots H_2O$, we only take into account that the glyoxal approaches near the formed $HO_2\cdots H_2O$ complex to elucidate the reaction mechanisms of glyoxal with the $HO_2\cdots H_2O$ complex relative to the atmosphere. There are five complexes located herein, whose stabilization energies are in the range of −9.3 to −12.3 kcal/mol from Table 1. Moreover, as the complexes C4, C6 and C7 are contributors on the reaction mechanisms of glyoxal with the $HO_2\cdots H_2O$ complex and their binding energies change slightly, the three complexes are mainly discussed below.

The complex C4 is a eight-membered ring structure containing the two hydrogen bonds and one van der Waals bond. It is worth noting that according to Steiner [49], the O10···H9 bond distance of 1.680 Å is the moderate interaction, reflecting the interaction in nature is mostly electrostatic and partially covalent, which is confirmed by the AIM analysis because of the total electron energy density with the value of −0.0045 au. In addition, the charge density at the O10H9 is 0.0469 au, which exceeds the upper limit value of charge density proposed by Koch and Popelier [50]. The complexes C6 and C7 are the nine-membered ring structure and the eight-membered ring structure with three hydrogen bonds included, which is a plane structure. In the two complexes, the interaction between O10 and H9 is dominated in terms of the geometrical parameters and topological analysis. However, the O7···H6 strengthen in complex C6 and the O7···H1 interaction in C7 are very weak because their bond distances are very long and their charge densities do not arrive at the lower limit of the value proposed by Koch and Popelier [50].

The ternary complexes C9, C10, C11 and C12 can also be formed by the interaction the HO_2 radical with the formed (CHO)2···H_2O complex as shown in Fig. 2. The binding energies of the complexes are calculated in the range of the −6.2 kcal/mol to −8.3 kcal/mol. It is noted that the complex C10 is more stable than the complexes C9, C11 and C12 because of the distances of the two hydrogen bonds between water and glyoxal 2.097 and 2.292 Angstroms, which are shorter than C9, C11, and C12. The binding energies of the complexes C9, C11 and C12 are slightly different, which is reasonably consistent with the corresponding geometrical structures. In addition, from the topological properties listed in Table 3, it is worth noting that the complexes C9 and C10 contain two ring structures, while the complexes C11 and C11 involve one ring structure.

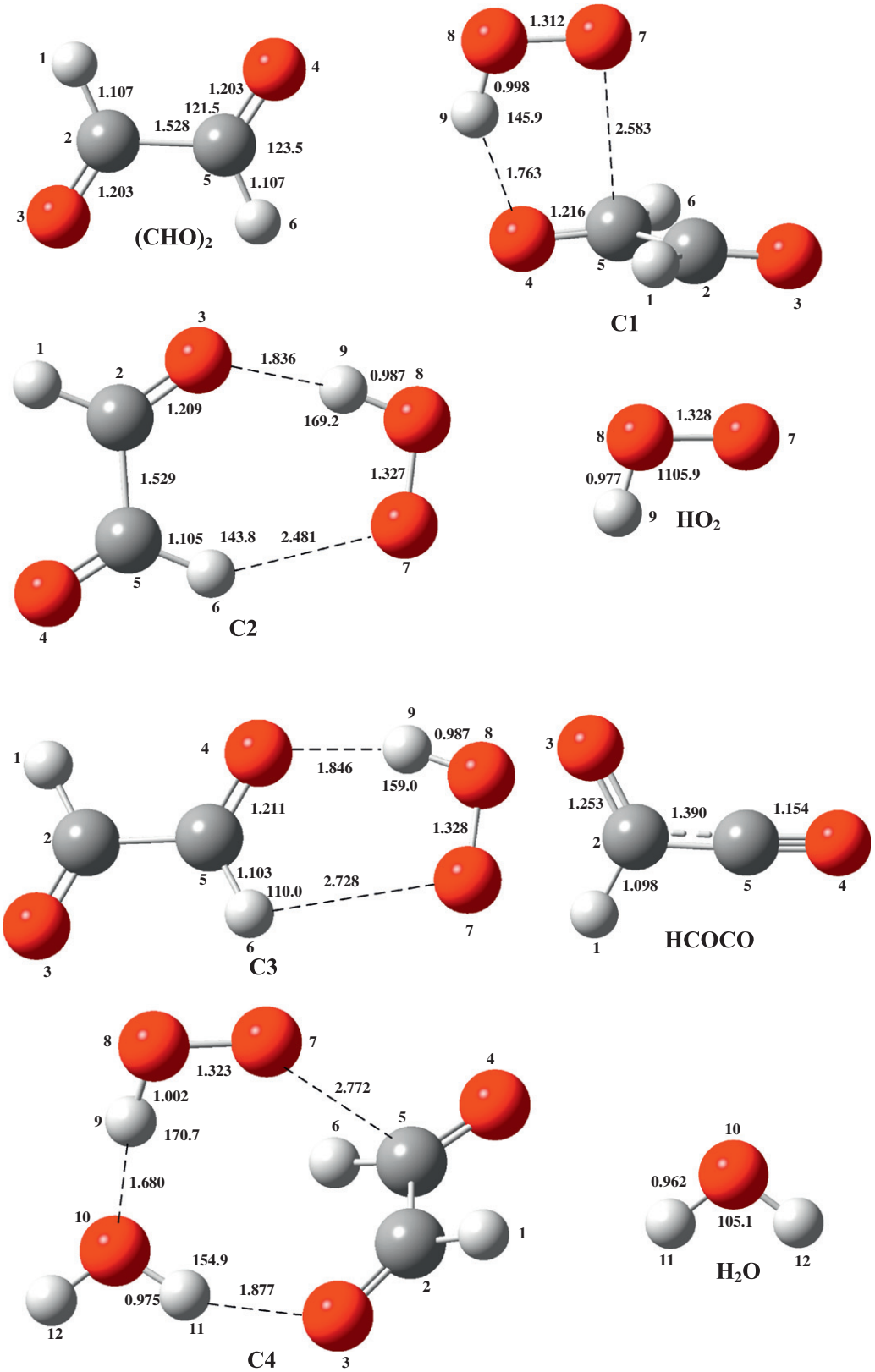

Fig. 1. The selected reactants, complexes and products at the B3LYP/6-311++G(d,p) level of theory (bond distances in angstroms and angles in degrees).

3.2. The reaction of glyoxal with HO_2

There are two types of reactions found herein with four different transition structures for the radical addition TS1 and TS4 and the hydrogen abstraction TS2 and TS3 in Fig. 3. The calculated potential energy profile clearly illustrates the dominant reaction mechanism as provided in Fig. 4. From Table 1, the calculated results show that the TS1 is preferable than other reaction

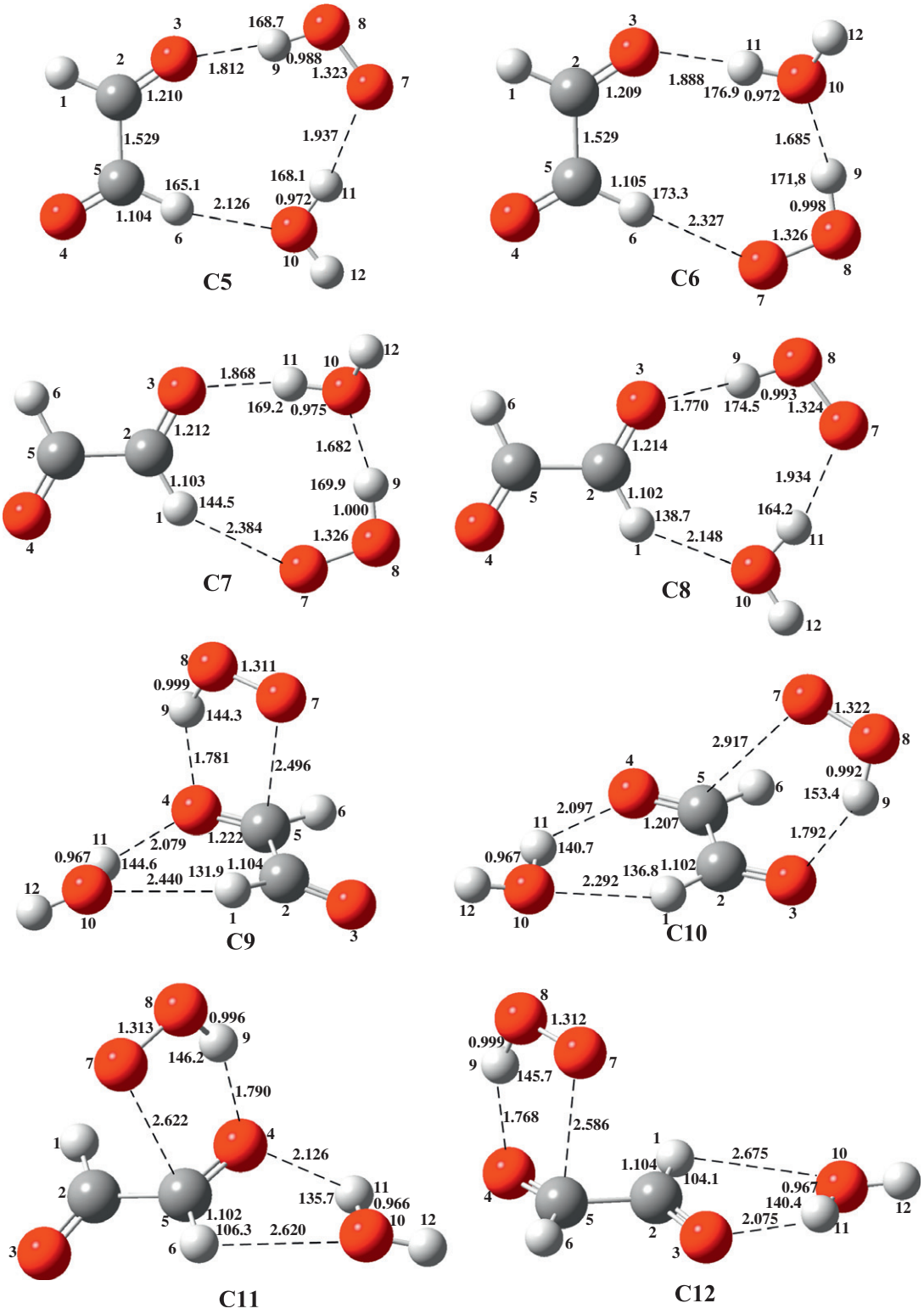

Fig. 2. The optimized complexes at the B3LYP/6-311++G(d,p) level of theory.

pathways. The transition state TS1 is a five-membered ring structure similar to the reaction of HO_2 and HCHO [26], which is described as the proton coupled electron transfer mechanism [51]. The H9 of HO_2 is transferred to O4 atom of glyoxal, simultaneously the terminal O7 of HO_2 atom is added to the C5 of the carbonyl group in glyoxal and the electron transfer occurred between two oxygen atoms of HO_2. The energy barrier is calculated to be 1.6 kcal/mol, 5.4 kcal/mol with respect to the free reactants and the pre-reactive complex C1, which is higher than the corresponding energy barriers of the reactions HO_2 with HCHO [26] and OH with glyoxal [45] by 3.7 kcal/mol, 5.0 kcal/mol relative to the separated reactants. Additionally, the reaction is exothermic with the value of $\Delta H = -11.2$ kcal/mol (see Table 1), which is 5.6 higher than the value in the corresponding reaction of HCHO with HO_2

Table 1
The Reaction and activated energies, enthalpies and free energies for the reactions $(CHO)_2$ with HO_2 and HO_2 with H_2O added with zero-point correction included at 298 K. (kcal/mol).

Compound	ΔH^c	ΔG^c	ΔE^a	ΔE^b	ΔE^c	T1[d]
$(CHO)_2 + HO_2$	0.0	0.0	0.0	0.0	0.0	0.017,0.030
C1	−4.1	5.6	−5.0	−4.6	−3.8	0.026
TS1	0.3	12.7	−1.7	1.6	1.6	0.028
HC(O)C(OO)OH (P1)	−11.2	0.3	−8.4	−10.2	−10.2	0.025
$(CHO)_2 + HO_2$	0.0	0.0	0.0	0.0	0.0	0.017,0.030
C2	−5.2	3.6	−5.6	−5.8	−5.2	0.025
TS2	14.4	23.7	9.4	14.7	14.7	0.028
C3	−5.4	3.1	−5.5	−6.0	−5.4	0.025
TS3	15.0	23.9	9.4	15.1	15.1	0.027
$HCOCO(P2)+H_2O_2$	3.7	3.5	−1.4	3.5	3.5	0.031,0.013
$(CHO)_2 + HO_2$	0.0	0.0	0.0	0.0	0.0	0.017,0.030
TS4	18.2	30.1	11.7	19.1	19.1	0.047
HCOHC(OOH)O(P3)	6.1	17.3	4.1	6.8	6.8	0.032
$(CHO)_2 + HO_2 + H_2O$	0.0	0.0	0.0	0.0	0.0	0.017,0.030,0.011
C4	−13.0	5.3	−13.2	−14.2	−12.3	0.024
TS5	2.9	25.5	−0.9	5.2	5.2	0.022
C5	−9.5	7.0	−10.4	−10.5	−9.3	0.023
C6	−12.2	4.6	−13.1	13.4	−11.8	0.023
TS6	6.8	25.7	2.2	7.6	7.6	0.026
C7	−12.6	4.7	−13.3	−13.6	−12.0	0.023
TS7	8.9	26.9	3.7	9.5	9.5	0.027
C8	−10.4	6.6	−11.3	−11.3	−10.1	0.023
C9	−6.6	11.0	−7.2	−7.6	−6.2	0.024
TS8	−3.8	16.3	−4.1	−2.4	−2.4	0.025
C10	−8.6	8.3	−8.6	−9.5	−8.3	0.023
TS9	−4.0	16.3	−5.3	−2.6	−2.6	0.026
C11	−6.8	8.6	−7.0	−7.8	−6.6	0.024
TS10	−3.6	15.8	−3.8	−2.3	−2.3	0.025
C12	−7.1	7.9	−7.6	−7.9	−6.8	0.024
TS11	−3.0	16.1	−4.5	−1.8	−1.8	0.025
$(CHO)_2 + H_2O$	0.0	0.0	0.0	0.0	0.0	0.017,0.011
Pre-1-1	−3.2	3.6	−3.1	−3.5	−3.1	0.016
Pre-2-1	−2.8	3.9	−2.5	−3.1	−2.8	0.016

[a] ΔE are computed at the B3LYP/6-311++G(d,p) level of theory.
[b] ΔE is calculated at the CCSD(T)//B3LYP/6-311++G(d,p) level of theory.
[c] The values are computed at the CCSD(T)//B3LYP/6-311++G(d,p) level of theory plus the BSSE correction at the B3LYP/6-311++G(d,p) level of theory.
[d] T1 is diagnostic value.

[26]. The energy difference between the reactions of HO_2 with HCHO and glyoxal could lead to the reaction $HO_2 + (HCO)_2$ more slowly. The terminal oxygen of HO_2 addition to the carbon atom of carbonyl group in glyoxal occurs via the transition state TS4 in Fig. 3 and there is no pre-reactive complex found for the elementary process. The activated barrier is computed to be 19.1 kcal/mol, which is so high that the process is unlikely to occur in the atmosphere.

The hydrogen atom of glyoxal abstracted by HO_2 takes place via the corresponding transition states TS2 and TS3, leading to the formation of the products HCOCO + H_2O_2. The calculated results demonstrate that the reaction is slightly endothermic with the value of ΔH = 3.7 kcal mol at the CCSD(T)//B3LYP/6-311++G(d,p) level of theory, which is in consistent with the formaldehyde abstracted by HO_2 [26]. The two different transition state structures are determined by the relative orientation of HOO moiety with respect to the carbonyl group of glyoxal. Additionally, the barriers of the two transition states are about 15.0 kcal/mol, 20.0 kcal/mol relative to the reactants and the corresponding pre-reactive complexes, revealing that the processes are of no importance.

3.3. The reaction of glyoxal with HO_2 and H_2O

As for the reaction of glyoxal with HO_2 and H_2O, the elementary processes occur via the reactions of glyoxal with the formed $HO_2\cdots H_2O$ complex or HO_2 with the formed $(CHO)_2\cdots H_2O$ complex. Three different transition states for the reaction of glyoxal with the formed $HO_2\cdots H_2O$ complex are located with one radical addition and two hydrogen abstractions as shown in Fig. 3. It is noted that the barriers of the three transition states (TS5, TS6 and TS7) are in the range of 17.5–21.5 kcal/mol relative to the respective pre-reactive complex, which indicates that the processes hamper the reaction $HO_2 + (CHO)_2$. However, it is pointed out that the water-assisted proton coupled electron transfer is of great interest because the concentration of the complex $HO_2\cdots H_2O$ is very high in the atmosphere. In addition, it is obvious that the TS5 is the main reaction channel for the energetic point of view, reflecting the reaction mechanisms of the reactions of HO_2 with glyoxal and glyoxal with the formed $HO_2\cdots H_2O$ complex are consistent.

According to the results above, the main reaction pathway of the $HO_2 + (HCO)_2$ occurs via TS1. Thus, when the HO_2 reaction with the formed $(CHO)_2\cdots H_2O$ complex is investigated, the proton coupled electron transfer mechanism is considered herein. Furthermore, due to two complexes formed between glyoxal with water [45] as shown in Fig. S1 supplementary material, there are four transition states located as shown in Fig. 5. From Table 1, the calculated barriers are 3.8 kcal/mol–5.7 kcal/mol, −2.6 kcal/mol to −1.8 kcal/mol with respect to the respective pre-reactive complex and the separated reactants, indicating that except TS9, the single water molecule can decrease the activated barrier of the reaction of HO_2 with glyoxal. It is noted that the barrier is slightly lowered about 1 kcal/mol.

3.4. Kinetics

As the reactions start with the formation of the pre-reactive complexes before the transition sates and release the products,

Table 2
Topological properties of the bond critical points of the $(CHO)_2\cdots HO_2$, and $(CHO)_2\cdots HO_2\cdots H_2O$ complexes at the B3LYP/6-311++G(d,p) level of theory.

Compound	Bond/ring	r[a] (Å)	ρ (au)[b]	$\Delta^2\rho$ (au)[c]	G (au)[d]	V (au)[e]	H (au)[f]
C1	O4H9	1.763	0.0369	0.1228	0.0308	−0.0309	−0.0001
	C5O7	2.583	0.0207	0.0612	0.0145	−0.0137	0.0008
	(3,1)	–	0.0151	0.0760	0.0165	−0.0140	0.0025
C2	O3H9	1.836	0.0311	0.1084	0.0259	−0.0247	0.0011
	H6O7	2.481	0.0101	0.0276	0.0063	−0.0057	0.0006
	(3,1)	–	0.0045	0.0196	0.0040	−0.0031	0.0009
C3	O4H9	1.846	0.0314	0.1072	0.0260	−0.0252	0.0008
	C6O7	2.728	0.0068	0.0236	0.0051	−0.0043	0.0008
	(3,1)	–	0.0062	0.0284	0.0060	−0.0049	0.0011
C4	H9O10	1.680	0.0469	0.1400	0.0395	−0.0440	−0.0045
	H11O3	1.877	0.0275	0.1024	0.0235	−0.0214	0.0021
	C5O7	2.772	0.0125	0.0440	0.0094	−0.0078	0.0016
	(3,1)	–	0.0032	0.0160	0.0032	−0.0024	0.0008
C5	O3H9	1.812	0.0303	0.1164	0.0270	−0.0249	0.0021
	O7H11	1.937	0.0253	0.0900	0.0205	−0.0185	0.0020
	O10H6	2.126	0.0176	0.0636	0.0136	−0.0113	0.0023
	(3,1)	–	0.0015	0.0084	0.0015	−0.0009	0.0006
C6	O3H11	1.888	0.0258	0.1000	0.0224	−0.0198	0.0026
	O10H9	1.685	0.0456	0.1412	0.0391	−0.0429	−0.0038
	O7H6	2.327	0.0120	0.0360	0.0079	−0.0068	0.0011
	(3,1)	–	0.0016	0.0076	0.0013	−0.0007	0.0006
C7	O3H11	1.868	0.0285	0.1036	0.0241	−0.0223	0.0018
	O10H9	1.682	0.0465	0.1412	0.0395	−0.0437	−0.0042
	O7H1	2.384	0.0110	0.0336	0.0074	−0.0064	0.0010
	(3,1)	–	0.0024	0.0124	0.0023	−0.0015	0.0008
C8	O3H9	1.770	0.0363	0.1212	0.0305	−0.0307	−0.0002
	O7H11	1.934	0.0256	0.0896	0.0206	−0.0188	−0.0018
	O10H1	2.148	0.0173	0.0636	0.0136	−0.0113	0.0023
	(3,1)	–	0.0023	0.0132	0.0025	−0.0017	0.0008

[a] The distance of hydrogen bonding.
[b] Electronic charge density at the critical point.
[c] Laplacian of the electron density at the bond critical point.
[d] Kinetic electron density at the bond critical point.
[e] Potential electron energy density at the bond critical point.
[f] Total electron energy density at the bond critical point.

Table 3
Topological properties of the bond critical points of the $(CHO)_2\cdots HO_2\cdots H_2O$ complexes at the B3LYP/6-311++G(d,p) level of theory.

Compound	Bond/ring	r[a](Å)	ρ (au)[b]	$\Delta^2\rho$ (au)[c]	G (au)[d]	V (au)[e]	H (au)[f]
C9	O4H9	1.781	0.0360	0.1192	0.0297	−0.0296	0.0001
	C5O7	2.496	0.0242	0.0700	0.0169	−0.0163	0.0006
	O4C5O7O8H9	–	0.0160	0.0828	0.0180	−0.0153	0.0027
	O4H11	2.079	0.0186	0.0688	0.0150	−0.0128	0.0022
	O10H1	2.440	0.0095	0.032	0.0069	−0.0058	0.0011
	O4H11O10H1C2C5	–	0.0058	0.0268	0.0054	−0.0041	0.0013
C10	O3H9	1.792	0.0346	0.1176	0.0291	−0.0288	0.0003
	C5O7	2.917	0.0106	0.0372	0.0080	−0.0067	0.0013
	O2C2C5O7O8H9	–	0.0086	0.0340	0.0072	−0.0059	0.0013
	O4H11	2.097	0.0124	0.0444	0.0094	−0.0077	0.0017
	O10H1	2.292	0.0179	0.066	0.0143	−0.0121	0.0022
	O4H11O10H1C2C5	–	0.0064	0.0296	0.0061	−0.0048	0.0013
C11	O4H9	1.790	0.0348	0.1172	0.0289	−0.0285	0.0004
	C5O7	2.622	0.0193	0.0584	0.0136	−0.0126	0.001
	O4C5O7O8H9	–	0.0142	0.0708	0.0154	−0.0131	0.0023
	O4H11	2.126	0.0173	0.0636	0.0139	−0.0119	0.002
C12	O4H9	1.768	0.0365	0.1208	0.0303	−0.0304	−0.0001
	C5O7	2.586	0.0207	0.0612	0.0145	−0.0137	0.0008
	O4C5O7O8H9	–	0.0150	0.0752	0.0164	−0.0140	0.0024
	O3H11	2.075	0.0188	0.0696	0.0152	−0.0130	0.0022

[a] The distance of hydrogen bonding.
[b] Electronic charge density at the critical point.
[c] Laplacian of the electron density at the bond critical point.
[d] Kinetic electron density at the bond critical point.
[e] Potential electron energy density at the bond critical point.
[f] Total electron energy density at the bond critical point.

the reaction mechanism can be characterized by the Eq. (1). Assuming that the pre-reactive complex is in equilibrium with the reactants and in terms of the steady-state conditions, the rate constant is expressed as

$$(HCO)_2 + HO_2 \underset{k_{-1}}{\overset{k}{\leftrightarrow}} \text{Pre-reactive Complex} \xrightarrow{k_2} \text{Products} \quad (1)$$

$$k = \frac{k_1}{k_{-1}} k_2 = K_{eq} k_2 \quad (2)$$

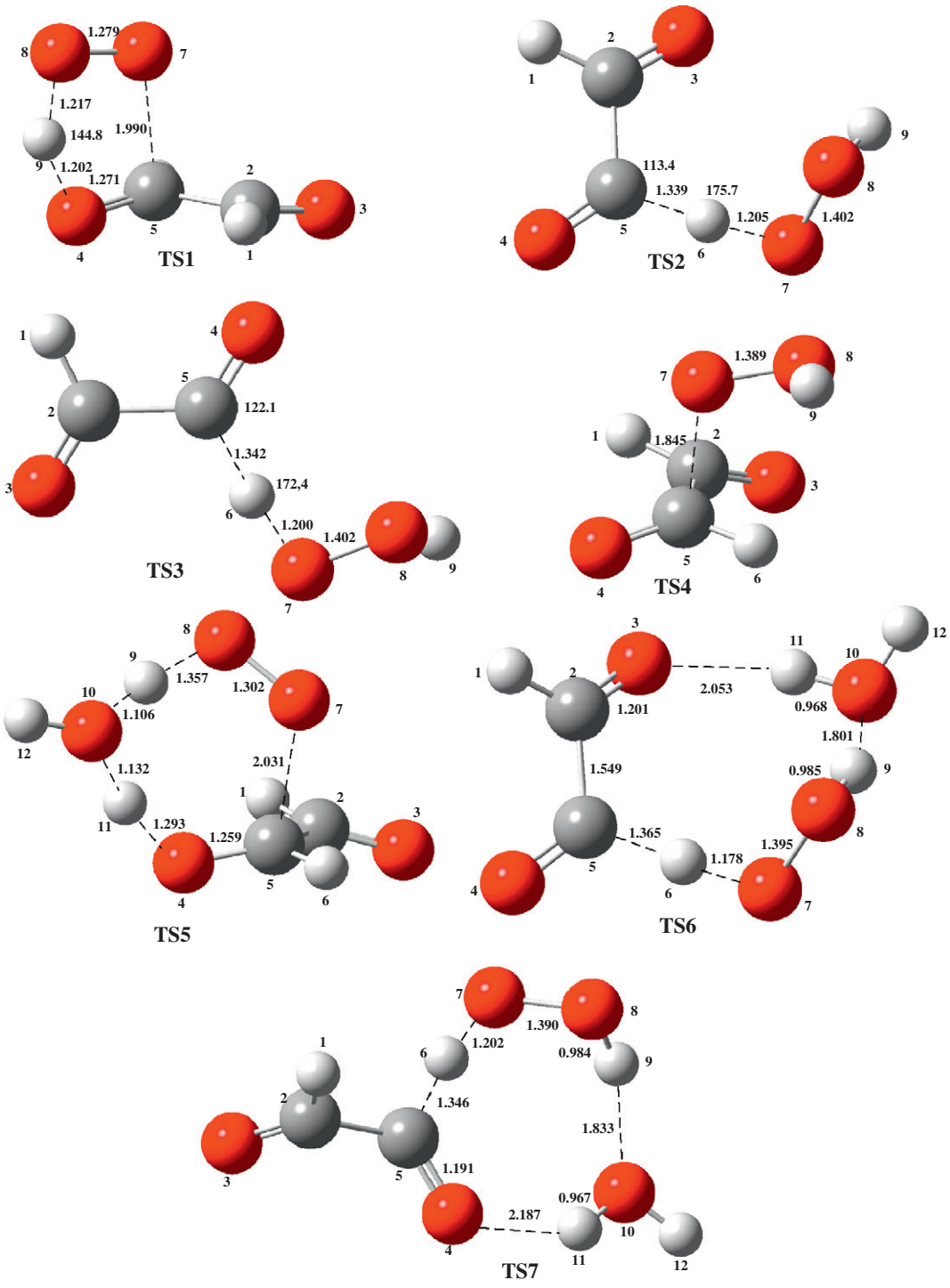

Fig. 3. The optimized transition states at the B3LYP/6-311++G(d,p) level of theory.

The K_{eq} and k_2 are the equilibrium constant of the first step and the rate constant of the second step in the reactions respectively, which is calculated by the following equations:

$$K_{eq}(T) = \sigma \frac{Q_{complex}}{Q_R} \exp[-(E_C - E_R)/RT] \quad (3)$$

$$k_2(T) = \kappa\sigma \frac{k_B T}{h} \frac{Q_{TS}}{Q_{complex}} \exp[-(E_{TS} - E_c)/RT] \quad (4)$$

where Q_{TS}, Q_R and Q_c denote the partition functions of the transition states, the reactants and the pre-reactive complex, k_B is the Boltzmann's constant, κ is the transmission coefficient and σ is the symmetry factor. The E_{TS}, E_R and E_c stand for the total energy of the transition states, the reactants and the complexes with zero point energy correction involved.

For simplicity, as the computed results show that the main reaction pathways in the reactions of glyoxal with HO_2 glyoxal and H_2O and HO_2 are the TS1 and TS8-TS11 and other reaction paths are not possible to take place because of the high activated barriers in the atmosphere. Thus, the rate constants via TS1 and TS8-TS11 are calculated as listed in Table 4. The rate constant via TS1 is found to be 2.83×10^{-16} cm^3 molecule^{-1} s^{-1} at 298 K, which compares well with the experimental results [25], demonstrating

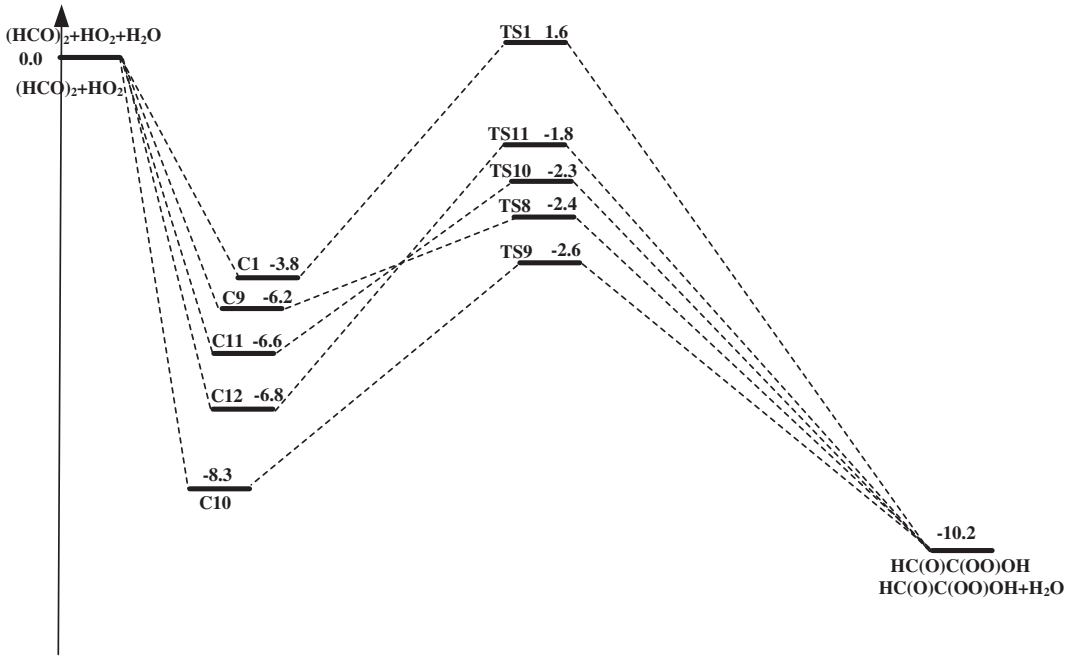

Fig. 4. The calculated potential energy profile of the main reaction pathways for the reaction of glyoxal with HO_2 and HO_2 with H_2O added at the CCSD(T)//B3LYP/6-311++G(d,p) level of theory (kcal/mol).

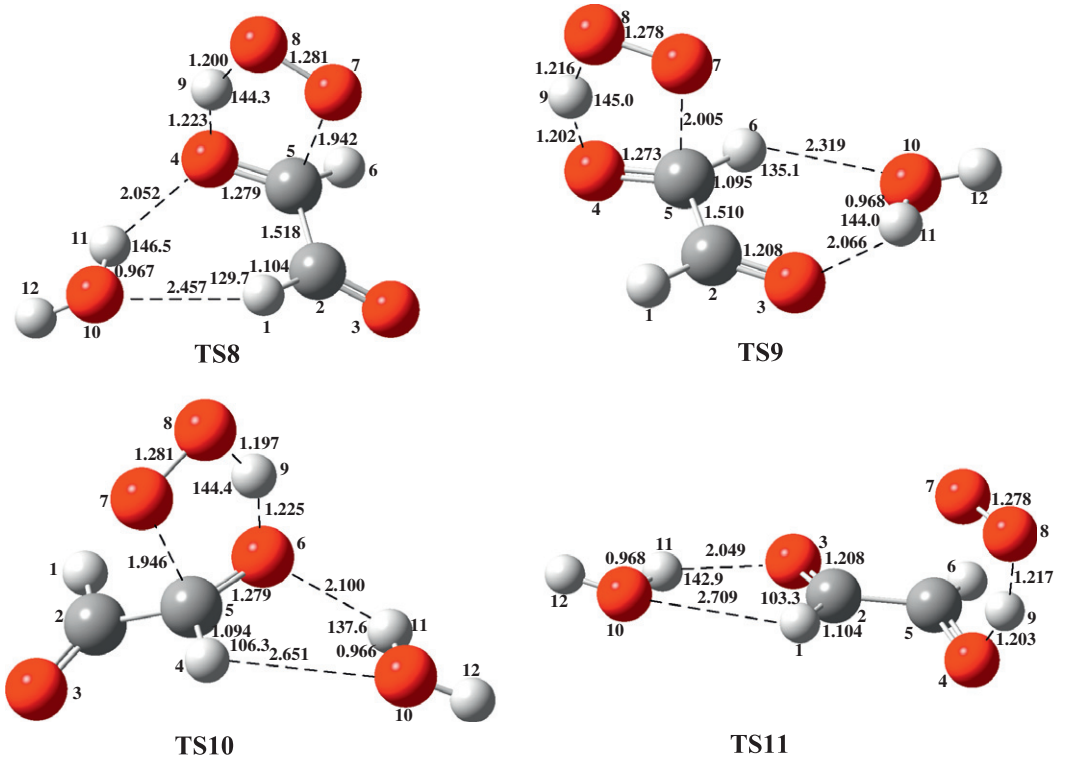

Fig. 5. The optimized transition states at the B3LYP/6-311++G(d,p) level of theory.

that the theoretical methods used herein are reliable. As for the reaction $(HCO)_2 + HO_2$ in the atmosphere, the importance is limited because the rate constant of $(HCO)_2 + HO$ with the value of $(9.15 \pm 0.8) \times 10^{-12}$ cm^3 molecule^{-1} s^{-1} [52] is about 10^4 times greater than that of TS1 herein. Moreover, the ratio between HO_2 and OH is about 150. Therefore, the reaction reported herein is not competitive well with the reaction of glyoxal with HO. In addition, the calculated rate constants also show that the single water can increase the rate constant of the reaction $HO_2 + (CHO)_2$. However, from Table 4, via TS10, the rate is about 10 times faster than that of the naked $HO_2 + (CHO)_2$ reaction. To estimate the importance the reaction of glyoxal with HO_2 in the presence of water, the concentrations of the complexes between glyoxal and water are calculated in terms of the equilibrium constants of the complexes Pre-1-1 and Pre-2-1 and their concentrations in the atmosphere. The computed equilibrium constants K_{eq}(Pre-1-1)

Table 4
The calculated (k, cm^3 $molecule^{-1}$ s^{-1}) rate constant for the elementary process in the temperature range 260–320 K.

Reaction	260	270	280	290	298	310	320
TS1	2.57×10^{-16}	2.62×10^{-16}	2.68×10^{-16}	2.77×10^{-16}	2.83×10^{-16}	2.95×10^{-16}	3.05×10^{-16}
TS8	7.53×10^{-16}	7.27×10^{-16}	7.06×10^{-16}	6.91×10^{-16}	6.81×10^{-16}	6.70×10^{-16}	6.64×10^{-16}
TS9	8.66×10^{-16}	8.18×10^{-16}	7.80×10^{-16}	7.49×10^{-16}	7.29×10^{-16}	7.06×10^{-16}	6.91×10^{-16}
TS10	2.40×10^{-15}	2.28×10^{-15}	2.19×10^{-15}	2.12×10^{-15}	2.07×10^{-15}	2.02×10^{-15}	1.98×10^{-15}
TS11	1.56×10^{-15}	1.53×10^{-15}	1.51×10^{-15}	1.50×10^{-15}	1.49×10^{-15}	1.50×10^{-15}	1.50×10^{-15}

and K_{eq}(Pre-2-1) are 5.08×10^{-23} cm^3 $molecule^{-1}$, 2.68×10^{-23} cm^3 $molecule^{-1}$ at 298 K, respectively, which agrees well with the calculated results [53]. Considering the concentrations of glyoxal with the value of 2.46×10^{13} cm^3 $molecule^{-1}$ and water about 10^{17} cm^3 $molecule^{-1}$, the concentrations of the complex between glyoxal and water is less than 0.01% of the free glyoxal concentration. Thus, the water-assisted reaction of glyoxal with HO_2 is of no importance because it cannot be competitive well with the naked reaction $(CHO)_2 + HO_2$. The similar results are also reported on the reaction acetaldehyde + OH in the presence of water [54].

4. Conclusions

The reactions of glyoxal with HO_2 and HO_2 and H_2O are theoretically investigated, showing that there are four different transition states in the reaction $HO_2 + (HCO)_2$. The preferred reaction channel is the proton coupled electron transfer with the barrier of 5.4 kcal/mol with respect to pre-reactive complex, which is different from the reaction of OH with glyoxal because the hydrogen atom of glyoxal abstracted by the OH radical is dominated. Additionally, the reaction via TS1 is very complex mechanism and takes place through the pre-reactive complex prior to the transition state TS1. In addition, the barrier of the reaction $HO_2\cdots H_2O + (HCO)_2$ is enhanced so high that the reaction does not occur in the atmosphere. However, the energy barrier of the HO_2 reaction with the formed $(CHO)_2\cdots H_2O$ complex is lowered about 1 kcal/mol comparing the naked HO_2 reaction with glyoxal. The calculated rate constant is 2.83×10^{-16} cm^3 $molecule^{-1}$ s^{-1}, which is in good agreement with experimental data [52]. The slow rate constant is due to the high activated barrier.

Acknowledgment

This project was supported by natural science foundation of Guizhou University for Nationalities (2010). The authors thank the anonymous referee for providing the valuable comments.

Appendix A. Supplementary material

Supplementary data associated with this article can be found, in the online version, at doi:10.1016/j.comptc.2011.01.003.

References

[1] J. Yu, H.E. Jeffries, R.M. Le Lacheur, Environ. Sci. Technol. 29 (1995) 1923.
[2] R. Volkamer, F. San Martini, L.T. Molina, D. Salcedo, J.L. Jimenez, M.J. Molina, Geophys. Res. Lett. 34 (2007) L19807.
[3] F. Wittrock, A. Richter, H. Oetjen, J.P. Burrows, M. Kanakidou, S. Myriokefalitakis, R. Volkamer, S. Beirle, U. Platt, T. Wagner, Geophys. Res. Lett. 33 (2006) L16804.
[4] P.B. Shepson, E.O. Edney, E.W. Corse, J. Phys. Chem. 88 (1984) 4122.
[5] H. Bandow, N. Washida, H.Bull. Akimoto, Chem. Soc. Jpn. 58 (1985) 2531.
[6] S. Beirle, R. Volkamer, F. Wittrock, A. Richter, J. Burrows, U. Platt, T. Wagner, Geophys. Res. Lett. 32 (2005) L11810.
[7] A.J. Kean, E. Grosjean, D. Grosjean, R.A. Harley, Environ. Sci. Technol. 35 (2001) 4198.
[8] E. Grosjean, P.G. Green, D. Grosjean, Anal. Chem. 71 (1999) 1851.
[9] R. Volkamer, P. Spietz, J. Burrows, U. Platt, J. Photochem. Photobiol. A 172 (2005) 35.
[10] W.P. Hastings, C.A. Koehler, E.L. Bailey, D.O. De Haan, Environ. Sci. Technol. 39 (2005) 8728.
[11] J.H. Kroll, N.L. Ng, S.M. Murphy, V. Varutbangkul, R.C. Flagan, J.H. Seinfeld, J, Geophys. Res. Atmos. 110 (2005) D23207.
[12] J. Liggio, S.M. Li, R.J. McLaren, Geophys. Res. Lett. 110 (2005) D10304.
[13] L.A. Corrigan, W.S. Hanley, D.O.D. Haan, Environ. Sci. Technol. 42 (2008) 4428–4433.
[14] D.O. De Haan, L.A. Corrigan, W.K. Smith, R.D. Dtroik, R.D. Stroik, J.J. Turley, E.F. Lee, A.M. Tolbert, L.J. Gimenez, E.K. Cordova, R.G. Ferreell, Environ. Sci. Technol. 43 (2009) 2818.
[15] C.N. Plum, E. Sanhueza, R. Atkinson, W.P.L. Carter, J.N. Pitts, Jr. Environ. Sci. Technol. 17 (1983) 479.
[16] G.K. Moortgat, Pure Appl. Chem. 73 (2001) 487.
[17] M. Colberg, G. Friedrichs, J. Phys. Chem. A. 110 (2006) 160.
[18] F.L. Nesbitt, J.F. Gleason, L.J. Stief, J. Phys. Chem. A. 103 (1999) 3038.
[19] J.R. Salter, A.M. Blitz, E.D. Heard, J.M. Pilling, W.P. Seakins, J. Phys. Chem. A. 113 (2009) 8278–8285.
[20] F. Schweitzer, L. Magi, P. Mirabel, C. George, J. Phys. Chem. A. 102 (1998) 593.
[21] K. Matsumoto, S. Kawai, M. Igawa, Atmos. Environ. 39 (2005) 7321.
[22] M. Igawa, J.W. Munger, M.R. Hoffmann, Environ. Sci. Technol. 23 (1989) 556.
[23] J.W. Munger, D.J. Jacob, B.C. Daube, L.W. Horowitz, W.C. Keene, B.G. Heikes, J. Geophys. Res. 100 (1995) 9325.
[24] J. Kua, W.S. Hanley, D.O.D. Haan, J. Phys. Chem. A. 112 (2008) 66.
[25] H. Niki, P.D. Maker, C.M. Savage, L.P. Breitenbach, Int. J. Chem. Kinet. 17 (1985) 547.
[26] J.M. Anglada, V.M. Domingo, J. Phys. Chem. A 109 (2005) 10786.
[27] S. Aloisio, J.S. Francisco, J. Phys. Chem. A 102 (1998) 1899.
[28] S. Aloisio, J.S. Francisco, R.R. Friedl, J. Phys. Chem. A 104 (2000) 6597.
[29] R.S. Zhu, M.C. Lin, Chem. Phys. Lett. 354 (2002) 217.
[30] J. Gonzalez, M. Torrent-Sucarrat, J.M. Anglada, Phys. Chem. Chem. Phys 12 (2010) 2116.
[31] B. Long, X.f. Tan, D.S. Ren, W.J. Zhang, Chem. Phys. Lett. 492 (2010) 214.
[32] M.J. Frisch, G.W. Trucks, H.B. Schlegel, G.E. Scuseria, M.A. Robb, J.R. Cheeseman, J.A. Montgomery Jr., T. Vreven, K.N. Kudin, J.C. Burant, J.M. Millam, S.S. Iyengar, J. Tomasi, V. Barone, B. Mennucci, M. Cossi, G. Scalmani, N. Rega, G.A. Petersson, H. Nakatsuji, M. Hada, M. Ehara, K. Toyota, R. Fukuda, J. Hasegawa, M. Ishida, T. Nakajima, Y. Honda, O. Kitao, H. Nakai, M. Klene, X. Li, J.E. Knox, H.P. Hratchian, J.B. Cross, C. Adamo, J. Jaramillo, R. Gomperts, R.E. Stratmann, O. Yazyev, A.J. Austin, R. Cammi, C. Pomelli, J.W. Ochterski, P.Y. Ayala, K. Morokuma, G.A. Voth, P. Salvador, J.J. Dannenberg, V.G. Zakrzewski, S. Dapprich, A.D. Daniels, M.C. Strain, O. Farkas, D.K. Malick, A.D. Rabuck, K. Raghavachari, J.B. Foresman, J.V. Ortiz, Q. Cui, A.G. Baboul, S. Clifford, J. Cioslowski, B.B. Stefanov, G. Liu, A. Liashenko, P. Piskorz, I. Komaromi, R.L. Martin, D.J. Fox, T. Keith, M.A. Al-Laham, C.Y. Peng, A. Nanayakkara, M. Challacombe, P.M.W. Gill, B. Johnson, W. Chen, M.W. Wong, C. Gonzalez, J.A. Pople, Gaussian 03, Revision A, 01, Gaussian, Inc., Pittsburgh PA, 2003.
[33] T.J. Lee, P.R. Taylor, T1, Diag, Int. J. Quantum Chem. Symp. 23 (1989) 199.
[34] J.C. Rienstra-Kiracofe, W.D. Allen, H.F. Schaefer, J. Phys. Chem. A. 104 (2000) 9823.
[35] S.F. Boys, F. Bernardi, Mol. Phys. 19 (1970) 553.
[36] R.F.W. Bader, Chem. Rev. 91 (1991) 893.
[37] F. Biegler-Konig, J. Comput. Chem. 21 (2000) 1040.
[38] F. Biegler-Konig, J. Schonbohm, D. Bayles, J. Comput. Chem. 22 (2001) 545.
[39] F. Biegler-Konig, J. Schonbohm, J. Comput. Chem. 23 (2002) 1489.
[40] C. Gonzalez, H.B. Schelgel, J. Phys. Chem. 94 (1990) 5523.
[41] C. Gonzalez, H.B. Schlegel, J. Phys. Chem. 90 (1989) 2154.
[42] W.T. Duncan, T.N. Troung, 2000, <http://therate.hec.utah.edu> (accessed September 2000).
[43] G. Herzberg, Electronic Spectra and Electronic Structure of Polyatoci Molecules, Van Nostrand Reinhold Co., New York, 1966.
[44] K. Kuchltsul, T. Fukuyama, Y. Morino, J. Mol. Struct. 1 (1968) 463.
[45] B. Long, X.F. Tan, D.S. Ren, W.J. Zhang, J. Mol. Struct: Theochem. 956 (2010) 44.
[46] A. Galano, J.R. Alvarez-Idaboy, M.E. Ruiz-Santoyo, A. Vivier-Bunge, Chem. Phys. Chem. 5 (2004) 1379.
[47] R.F.W. Bader, Atom in Molecules: A Quantum Theory, Clarendon, Oxford, 1990.
[48] S. Aloisio, J.S. Francisco, J. Phys. Chem. A. 107 (2003) 2492.
[49] T. Steiner, Angew. Chem. Int. Ed. 41 (2002) 48.
[50] U. Koch, P.L. Popelier, J. Phys. Chem. 99 (1995) 9747.
[51] S. Olivella, J.M. Anglada, A. Sole, J.M. Bofill, Chem.-Eur. J. 10 (2004) 3404.
[52] K.J. Feierabend, L. Zhu, R.K. Talukdar, J.B. Burkholder, J, Phys. Chem. A. 112 (2007) 73.
[53] C. Iuga, J.R. Alvarez-Idaboy, A. Vivier-Bunge, Chem. Phys. Lett. 510 (2010) 11.
[54] C. Iuga, J.R. Alvarez-Idaboy, L. Reyes, A. Vivier-Bunge, J. Phys. Chem. Lett. 1 (2010) 3112.